Composites Science and Technology 137 (2016) 60–68

Contents lists available at ScienceDirect

Composites Science and Technology

journal homepage: http://www.elsevier.com/locate/compscitech

Synthesis and characterization of lignin carbon fiber and composites

Nathan Meek [a], Dayakar Penumadu [a, *], Omid Hosseinaei [b], David Harper [b], Stephen Young [a], Timothy Rials [b]

[a] Civil and Environmental Engineering, University of Tennessee at Knoxville, 325 John D Tickle Building, Knoxville, TN 37996, USA
[b] Center for Renewable Carbon, University of Tennessee at Knoxville, 2506 Jacob Drive, Knoxville, TN 37996, USA

ARTICLE INFO

Article history:
Received 3 June 2016
Received in revised form
18 October 2016
Accepted 19 October 2016
Available online 21 October 2016

Keywords:
Lignin
Carbon fibers
Biocomposites
Interface/interphase
Mechanical properties
Vacuum infusion

ABSTRACT

In this study, continuous lignin fibers from switchgrass have been successfully synthesized via multi-filament melt-spinning and converted to carbon fibers using optimized stabilization and carbonization techniques. Unidirectional lignin carbon fiber reinforced composites are produced using a vacuum assisted resin transfer molding process for the first time. Produced lignin carbon fiber is evaluated in mechanical, interfacial, and microstructural areas. Single fiber mechanical properties are characterized using a unique MTS Bionix Nano-UTM. Interfacial properties and resin/fiber behavior are evaluated using single fiber fragmentation. Microstructural properties are determined using wide-angle x-ray diffraction. Mechanical results indicated an initial tensile modulus along fiber axis of 36 GPa and a failure stress of 600 MPa for single carbon fibers. Lignin carbon fibers demonstrate a nonlinear increase in modulus with applied tensile strain similar to recently observed for commercial poly-acrylonitrile (PAN) carbon fibers. Microscopy revealed few defects within and along the lignin carbon fibers, and the processed lignin fibers demonstrated minimal crystalline regions and crystallite alignment when compared to commercial PAN based fibers. Interfacial shear strength with epoxy resin was found to be 17 MPa with a fiber fracture length of 228 μm. Unidirectional composite coupons achieved tensile modulus of 9 GPa and a failure strength of 85 MPa at 1% failure strain. Lignin carbon fiber and composites produced are targeted for non-structural applications as mechanical properties are currently less than PAN carbon fibers and therefore are not suitable to replace PAN carbon fiber at this stage. Relatively low composite strength is the likely result of fiber layup, fiber fusing, and non-continuous fibers across the gage length of the composite. Nano-tensile and interface shear strength results presented here have important implications for lignin carbon fiber composite development to optimize fiber/resin bonding. In addition, composite manufacturing procedures detailed here are a major step forward in the development of sustainable carbon fiber composite production.

1. Introduction

Carbon fiber composites due to their high strength to weight ratio are of interest to a wide range of industries including wind energy, aerospace, and automotive. Carbon-fiber reinforced polymers (CFRP) are of particular interest to the automotive industry because of recent US legislation requiring increased fuel economies of 35.5 mpg for 2017 and 54.5 mpg for 2025 [1]. It is estimated that CFRP's could reduce the weight of a car by 60%, which will dramatically increase fuel economy. Automotive companies are reluctant to switch to CFRP due to the high initial cost of materials [2]. This has led to a large effort to explore options for manufacturing inexpensive carbon fiber.

A large portion of the overall cost of carbon fiber based composites comes from the development and processing of the precursor to make the reinforcement. Most carbon fibers used for commercial and industrial applications comes from petroleum-based precursors such as polyacrylonitrile (PAN) and mesophase pitch (MPP). These precursors are relatively expensive and contribute to more than 50% of the manufacturing costs of a carbon fiber. Several other polymers, such as lignin and silk, have been targeted as possible replacements for carbon fiber precursors [3]. There is a growing interest in lignin, due to its potential abundance, high carbon content, renewable nature, and low cost as a by-product of the paper industry and biofuel extraction processes. Lignin, a complex, three-dimensional network polymer, is

* Corresponding author.
E-mail address: dpenumad@utk.edu (D. Penumadu).

http://dx.doi.org/10.1016/j.compscitech.2016.10.016
0266-3538/

comprised of aromatic alcohols with differing degrees of methoxy substitution based on parent plant material.

In this paper, authors use a modified organosolv fractionation process to produce lignin from an emerging bioenergy crop, switchgrass, which possesses high purity and desirable flow/rheological/extrusion characteristics for fiber processing [5–7]. Results reported in this paper are: (1) synthesis of organosolv fractionated lignin fibers, (2) suitable steps to stabilize and carbonize them, and (3) characterization techniques to determine mechanical, interfacial, and structural parameters. Important structure-property relationship associated with the mechanical behavior of the single fibers subjected to tensile loading was determined using a highly precise nano-tensile testing system. Carbonized fibers were characterized using x-ray diffraction (XRD) for crystallinity, and scanning electron microscopy (SEM) for morphology. Using 100% lignin based carbon fibers, quasi-isotropic Vacuum Assisted Resin Transfer Molding (VARTM) bio-epoxy based composites were also produced and mechanical properties were evaluated utilizing three dimensional digital image correlation (3D-DIC) to identify failure modes corresponding to these switchgrass based lignin composite panels produced for the first time by the authors.

2. Materials and methods

2.1. Lignin biomass and fiber production

The lignin used for the production of carbon fiber consisted of Alamo switchgrass (*Panicum virgatum*) feedstock supplied by TennEra, LLC. The lignin was isolated using a proprietary organosolv process resulting with high purity (98.1%) and low ash (0.12%) [4]. The lignin biomass was characterized using a Fisher-Johns melting point apparatus and Perkin Elmer Pyris 1 TGA [5–8]. The as-received switchgrass feedstock had a zero shear melt flow temperature (T_m) of ~170 °C observed and a glass transition temperature (T_g) of 109 °C. TGA results demonstrated that the lignin biomass contained an average of 6% moisture and began degrading in the 230–260 °C range.

Switchgrass lignin was melt-spun into fiber form using a pilot scale single-screw, pressure-controlled extruder (Alex James and Associates, Inc.), with temperature varied along the extruder barrel starting at 150–180 °C at the die and optimized for a residence time on the order of several minutes. Initially, lignin was pelletized using a 19 mm diameter extruder attached to a metering pump with a 15 mm orifice. Extrudate was quite brittle and pelletized before final extrusion into spun fibers. Pellets were dried in a vacuum oven at 80 °C and 560 mmHg for 12 h and subsequently melt-spun into fibers using a spinneret with twelve 150 μm diameter holes. Extruded green fibers (20–35 μm is diameter) were collected onto a winder at a take-up speed 300 m/min. The lignin fibers were mounted on steel meshes and placed in a programmable convection oven and oxidatively stabilized using a rate of 0.02 °C/min up to 250 °C. Stabilized fibers were transferred to a carbonization furnace where they were carbonized in a nitrogen environment at 3 °C/min to 1000 °C and held for 15 min. Produced carbon fiber possessed a near circular cross-section and were relatively defect free based on observations using scanning electron microscopy at various locations along the length of the fiber (Fig. 1). The average fiber diameter was 16.3 μm with a standard deviation of 5.7 μm.

2.2. Material selection for carbon fiber reinforced composite panel manufacturing

Super Sap Epoxy 100/1000 resin (Entropy Resins) consisting of epoxidized pine oils, was used as the matrix resin for carbon fiber composite panels due to its large biomass content (37% biobased carbon content from pine-based feedstocks) relative to other commercially available epoxies with the future goal of producing high biomass and sustainable composites. The curing agent for the Super Sap 100/1000 resin is benzyl alcohol and the resin is mixed 2:1 resin and hardener [9].

Carbon fiber composites composed of six plies, approximately 13 cm × 13 cm square, were produced in this study using a modified Vacuum Assisted Resin Transfer Molding (VARTM) process (Fig. 2). Unidirectional mats were placed in a preform inside a VARTM system and produced into a composite. Composite samples were then trimmed and cut to lengths for evaluating mechanical properties [10].

2.3. Single carbon fiber mechanical characterization

The mechanical properties of the single carbon fibers were determined using a MTS Bionix Nano-Universal Testing Machine (Nano UTM) equipped with custom grips specifically designed to test single fibers. The Nano UTM is a unique apparatus due to its high accuracy and resolution as well as its ability to measure static and dynamic properties. Accuracy is maintained by a rigorous set of internal electronic and mechanical calibrations before testing. The resolution for measuring load and displacement with this unique testing system are on the order of an nN and nm, respectively. Nano UTM (Fig. 3) offers the ability to obtain monotonic stress-strain data while continuously measuring the complex modulus as a function of applied tensile strain with a nano-mechanical actuating transducer (NMAT) [11].

Single fibers were observed using optical microscopy to obtain the diameter prior to testing on the UTM. After evaluating tensile properties for a representative batch of single fibers (typically 20 to 25), a two-parameter Weibull distribution is employed to obtain the shape and scale parameters associated with the tensile behavior of these carbon fibers and used in the derivation of the interfacial shear strength [17].

2.4. Composite mechanical characterization

The produced composite was mechanically tested using a servo-hydraulic testing system (MTS-810) equipped with a 5 kip load cell at a rate of 0.5 mm/min. Tensile test samples are prepared and tested according to relevant composite ASTM standards [10]. During the deformation of the composite sample, digital image correlation (DIC) system was used for obtaining local spatial variation of axial strains associated with potential heterogeneities in composite layup and processing. The DIC system has 50 micro-strain resolution at 1 Hz using dual 29 mega-pixel cameras from Correlated Solutions.

2.5. Fiber/resin interface characterization

Interfacial properties were determined using single fiber fragmentation testing (SFFT) or single filament composite (SFC) where a single carbon fiber is embedded in a dogbone sample of resin [17]. SFFT was completed using a micro-load custom frame to apply tension to the SFC while observing fiber fractures in the composite *in-situ* under polarized microscopy. The procedure utilized in this study was developed based on prior art associated with the related standards and practices for SFFT [12–14].

Using a custom developed load frame for SFFT, fiber fractures and their evolution under high magnification and polarized light were observed until saturation was reached in a systematic and consistent fashion. The broken fiber lengths and delamination zones are measured at saturation *in-situ*. From the fiber lengths, the

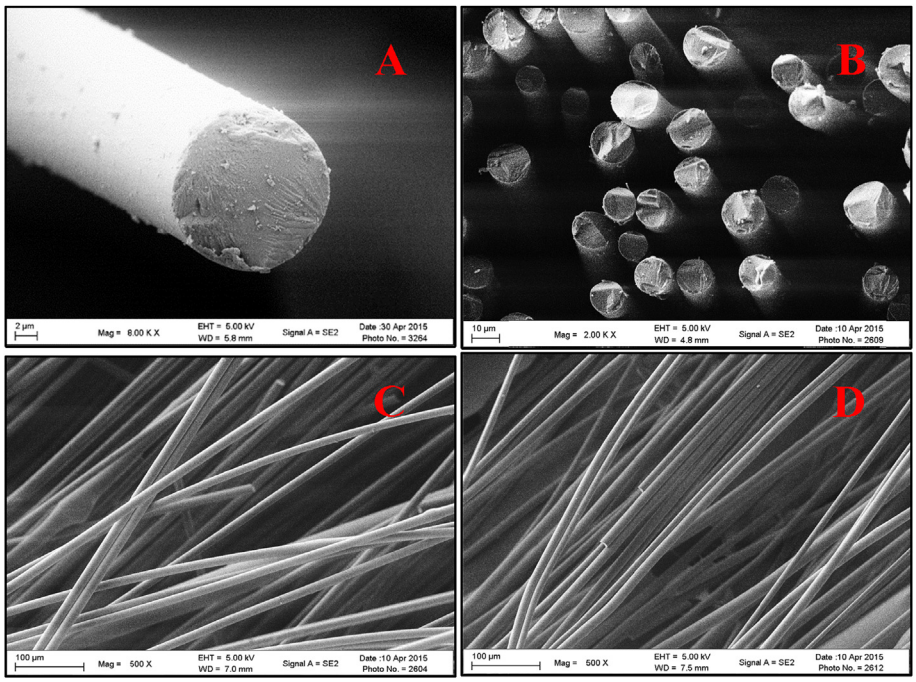

Fig. 1. (A) A SEM micrograph of a single carbon fiber, (B) cluster of carbon fibers showing the cross-sectional area of the fibers and void content. (C) and (D) SEM micrographs showing the surface morphology where fibers showed minimal defects.

interfacial shear strength (IFSS) is determined using Eq. (1):

$$\tau_{IFSS} = \frac{\sigma_f * d}{2 * l_c} \quad (1)$$

where τ_{IFSS} is the interfacial shear strength, σ_f is the tensile strength at given gauge length, d is the fiber diameters, and l_c is the critical fiber length.

2.6. Wide Angle X-Ray diffraction

Wide Angle X-Ray diffraction (WAXS) was completed on a Philips X'Pert XRD Diffractometer to evaluate the structure of the carbon fiber. Several parameters of interest to the lignin based carbon fibers include the peak positions corresponding to basal atomic planar spacing, the stacking height of the turbostratic graphitic planes (Lc), the crystallite size (La), and orientation of the planes with respect to the axis of the fiber, which are all important for structure-property relationships in PAN based carbon fibers [15–18]. The basal plane d-spacings of interest are the (002) and (100) as these indicate the crystallite parameters. Although normally the Lc and La are determined as well, the lignin carbon fiber showed little crystallinity; thus, these parameters are not considered.

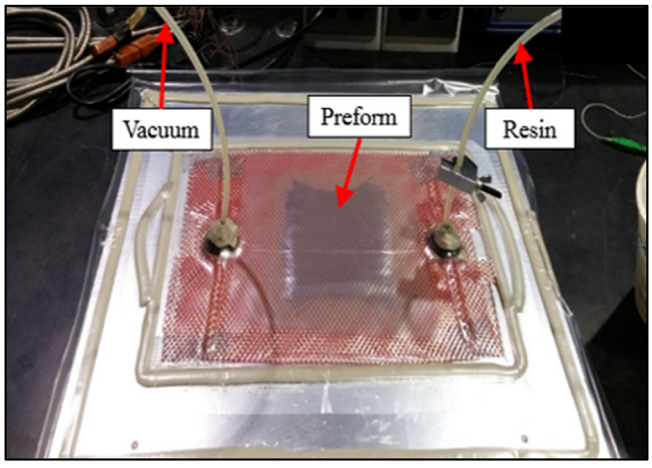

Fig. 2. The experimental set-up for resin infusion. The carbon fiber and preform can easily be seen in the middle of the set-up.

3. Results and discussion

3.1. Single fiber mechanical results

The single carbon fibers possessed an average failure stress of ~590 MPa and a tensile modulus of ~35 GPa (Table 1, Fig. 4). Compared to previous lignin based carbon fiber studies, the organosolv lignin fibers based on switchgrass biomass have favorable mechanical performance [2].

Fiber samples displayed a large variation in diameter due to difficulties during extrusion. Pressures and temperatures were varied to address extrudate properties during extrusion as it was difficult to produce consistent lignin fiber.

The tensile strength Weibull parameters from 27 single carbon fibers are 3.66 (m) and ~630 MPa (σ_0) for shape and scale parameters respectively (Fig. 4) which are developed to calculate the interfacial shear strength [19–22]. These parameters show a high scale parameter but lower shape parameter relative to other lignin Weibull parameters indicating higher strength lignin carbon fibers but a wider range of properties, probably due to variation in lignin molecule size from the feedstock after the fractionation process [23]. Relative to other current and past studies associated with attempts to develop carbon fibers from lignin precursors, these mechanical properties are relatively high [24,25]. In the authors' opinion, additional thermal treatments to improve the lignin-carbon structure and tensioning of the fibers during stabilization

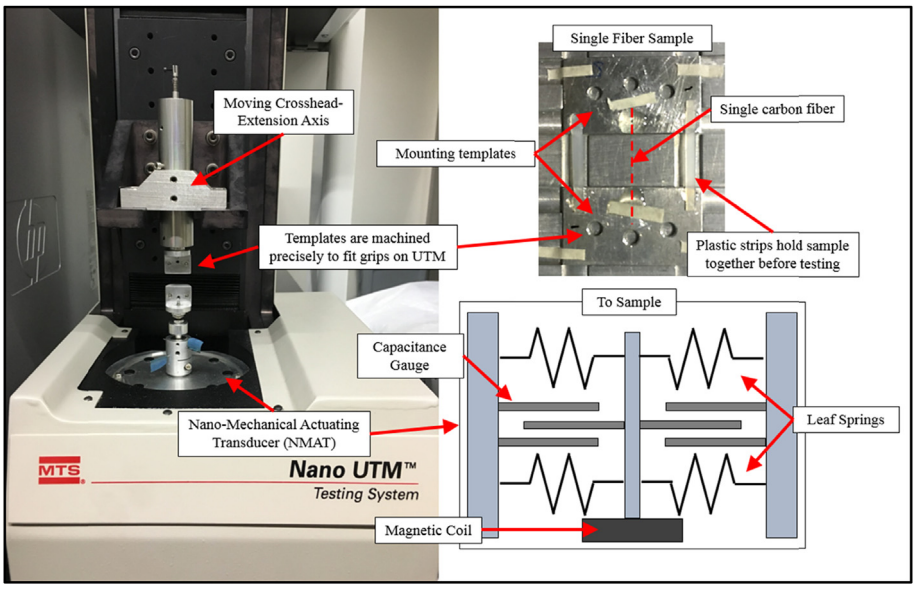

Fig. 3. The MTS-UTM testing apparatus (left). Mounted sample and schematic of the NMAT (right).

Table 1
Average single fiber mechanical results.

μ ± σ	Specimen Diameter	Modulus	Failure Strain	Failure Stress
# of Tests	um	GPa	mm/mm	MPa
27	16.2 ± 6.0	35.1 ± 6.1	0.017 ± 0.004	587 ± 192

and carbonization phase will likely reduce defect density with further improvements in mechanical properties and possibly also increase the crystalline regions thereby, increasing the effect of tensioning/alignment and mechanical properties [26].

As consistent with other reported literature, there is a correlation between fiber diameter and mechanical properties. As the fibers decrease in diameter the modulus increases due to a more effective stabilization process where oxidation of the fiber is easier with a smaller diameter [27]. From Fig. 5, it appears that a 5 μm fiber would have an approximate modulus of 36 GPa relative to 220 GPa standard modulus PAN carbon fiber [11]. The relationship of fiber diameter to modulus is not as well defined for lignin based carbon fibers relative to PAN based carbon fibers due to more variability in the lignin precursor fiber production process. Commercially available PAN carbon fibers are produced in highly controlled wet-spinning environments and there is a wealth of industrial experience for manufacturing PAN based fibers, therefore mechanical properties show less variation [11].

Interestingly, the lignin carbon fibers shows a nonlinear increase in modulus with tensile strain which is similar with PAN based carbon fiber samples [11]. PAN carbon fiber shows a distinct relationship between the initial tensile modulus value and its increase with applied axial strain as described in Eq. (2). Lignin carbon fiber exhibits similar non-linear stiffening behavior but to a lesser extent than was found for PAN based carbon fibers (Fig. 6).

$$E(\varepsilon) = (\gamma E_0) * \varepsilon + E_0 \quad (2)$$

In this equation, γE_0 is the change in modulus versus strain and E_0 is the initial storage modulus. PAN carbon fibers typically follow the equation [11]:

$$\gamma E_0 = 29.36 * E_0 - 1010 \quad (3)$$

This study has demonstrated that lignin carbon fibers adhere to this equation as well indicating that this equation may describe a universal feature of all carbon fiber (Fig. 6).

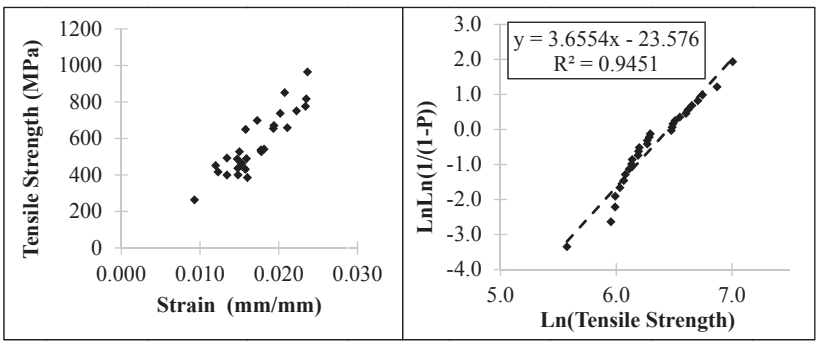

Fig. 4. (A) Failure stress vs strain for single fiber samples. (B) The Weibull distribution for the mechanical results of single fibers. The Weibull parameters determined are a shape parameter of 3.66 and scale parameter for ~630 MPa.

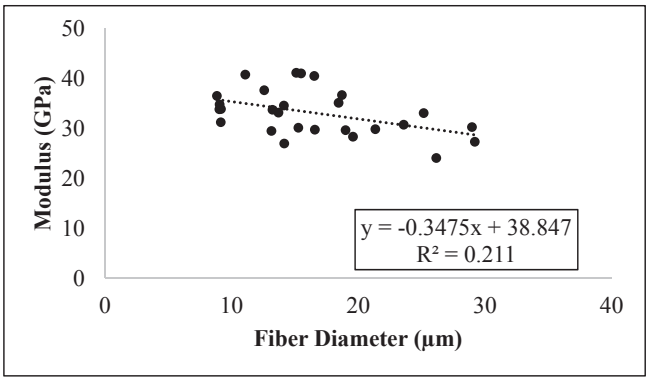

Fig. 5. Modulus versus fiber diameter. A linear trend-line was fitted to the data. The trend shows as fiber diameter gets smaller, the modulus tends to increase.

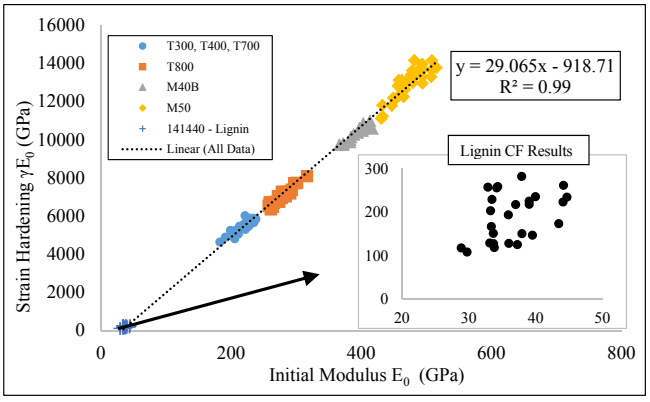

Fig. 6. Strain Hardening (Stiffening) vs. Initial Modulus from Kant and Penumadu [11] with additional lignin carbon fiber data. Inset: lignin carbon fiber data.

3.2. Amorphous microstructure

The wide-angle X-ray diffraction results for carbonized lignin fibers are shown in Fig. 7. Charts for evaluating the location of peaks near 26° and 43° 2θ, which are typically observed for PAN based carbon fibers, and the azimuthal scan about the (002) peak are shown. Little to no crystallinity can be observed for lignin-based carbon fibers based on these diffraction patterns. A fundamentally different microstructure develops in lignin-based carbon fibers compared to commercial PAN based fibers (Fig. 7). The diffraction analysis presented here is limited because the peaks are of low in intensity, full-width half-max (FWHM) is undeterminable, and results yield little crystalline structure information.

The highly amorphous microstructure is likely a result of the complex nature of the lignin molecule. Several factors limit the growth of crystalline regions within the lignin molecule during stabilization and oxidation including entanglements, heterogeneous molecular backbone, small phenolic groups not a part of the primary polymer chain, and contaminants. In comparison, PAN involves simple chemical modifications to obtain a turbostratic graphitic structure (dehydrogenation, cyclization, and carbonization) whereas the lignin molecule involves a multitude of different reactions and bonds to resemble a structure that is remotely similar to graphite [28,29] (Fig. 8).

3.3. Interfacial results

The ability of the fiber to transfer stress to the polymer matrix is governed by interfacial shear strength (IFSS) and is one of the most important parameters governing the strength of a fiber reinforced composites. Commercial PAN based carbon fibers undergo extensive surface treatment, including additional sizing, to provide a good interface with a target resin system, however, the fibers produced here have no surface treatments. In this study, the interfacial shear strength of unmodified lignin based carbon fibers with an epoxy resin system are reported for the first time (Table 2, Fig. 9). The SFFT results for the lignin carbon fiber indicate an interfacial shear stress of 16.7 MPa. Delamination zones tend to be nonexistent or quite small (~10 µm) due to the larger number of fractures along the fiber. This finding could be due to natural surface functionalization from lignin precursors.

The shape and size of the delamination zones suggest limited interfacial damage along the fiber during SFFT. The start of birefringent areas around a fiber fracture signal transfer of stress to the

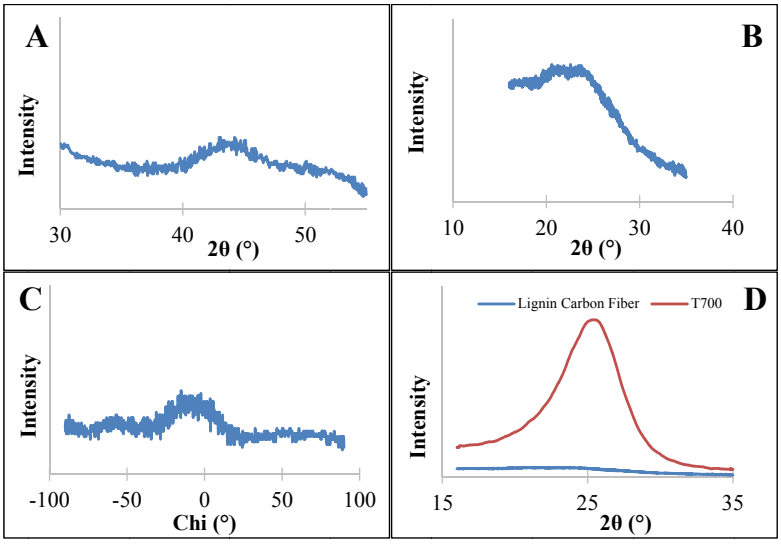

Fig. 7. (A) Diffraction pattern for the 2θ scan from 30 to 55°. (B) Diffraction pattern for the 2θ scan from 16 to 35°. (C) Diffraction pattern for the Chi scan from −90 to 90°. A small peak exists around 0° Chi indicating some orientation of the fiber. (D) Diffraction patterns for the Lignin Carbon Fiber and T700.

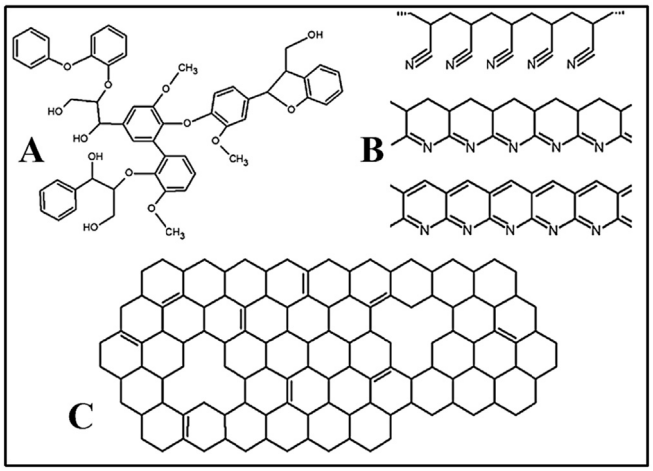

Fig. 8. (A) a simplified lignin molecule, (B) a PAN molecule with steps showing cyclization and dehydrogenation, and (C) a simplified plane of a turbostratic graphitic crystallite.

Table 2
The interfacial results for lignin carbon fiber.

μ ± σ	Fiber Length	IFSS
Measurements	μm	MPa
431	228.1 ± 109.3	16.7 ± 6.3

resin. Therefore, a gap between birefringent areas around a fiber fracture indicates delamination or fiber slippage [30]. Although the interface becomes damaged with increased strain, most fiber fractures tend to propagate into the resin signifying a strong interface with the lignin carbon fiber. Thus, while the IFSS is relatively high for no sizing applied to these lignin carbon fibers, at larger strains the fiber interface will become damaged instead of fully transferring stress into the matrix resin [31] (Fig. 9).

Another finding is that while interfacial damage occurs, the fiber does not pull out of the matrix, indicating the presence of significant interfacial shear strength with the epoxy resin system. Other fiber/resin systems that are commercially available with tailored sizing tend to show interfacial shear strengths in the range of 20–43 MPa [32,33]. Images from delamination zones (Fig. 9) illustrate significant bonding by propagating fractures into the matrix where the fibers fractures and large stressed regions signifying relatively effective stress transfer from untreated lignin carbon fiber to resin. Due to a lower carbonization temperature (1000 °C) employed in this study for producing lignin carbon fiber, it is likely that functional groups, such as hydroxyl, methoxyl groups, remain on the surface leading to a higher IFSS observed [34,35].

Additional improvements to the manufacturing process of these lignin based carbon fibers such as optimal stabilization and carbonization, possible integration of suitable sizing agents, improved fiber properties should further enhance IFSS and resulting reinforced composite properties. A significant factor that affects interface shear stress is the tensile strength of the carbon fiber and increasing lignin carbon fibers strength properties will further enhance its interface shear properties, an important finding for optimizing future lignin carbon fiber reinforced composite systems. Due to its relatively high interfacial shear strength for unsized carbon fiber, the lignin carbon fiber produced in this study would be ideal for various applications that take advantage of carbon fiber interfacial properties such as chopped fiber composites.

3.4. Mechanical behavior of lignin based carbon fiber composites

A reinforced composite laminate using the lignin carbon fibers was manufactured using VARTM resulted in a 14 cm by 14 cm panel as shown in Fig. 10 (a). The composite was then trimmed to 13 cm by 13 cm using a diamond blade saw. The trimmed composite possessed somewhat consistent density (3.43 ± 0.07 kg/m^2) and uniform thickness (0.2 ± 0.02 cm) across the sample (Fig. 10 (b)).

High-resolution strain mapping through three-dimensional digital image correlation (DIC) was used to identify local tensile strain deformation on the surface of the fabricated composite. Samples were cut to 100 cm by 12.5 cm [10] and GS10 glass fiber tabs were attached (Fig. 11). The samples are speckled with a random pattern as DIC maps strain by tracking relative displacements in the applied random speckle pattern on the sample during deformation. Table 3 shows the results collected from DIC and tensile testing of along fiber axis samples of the square laminates.

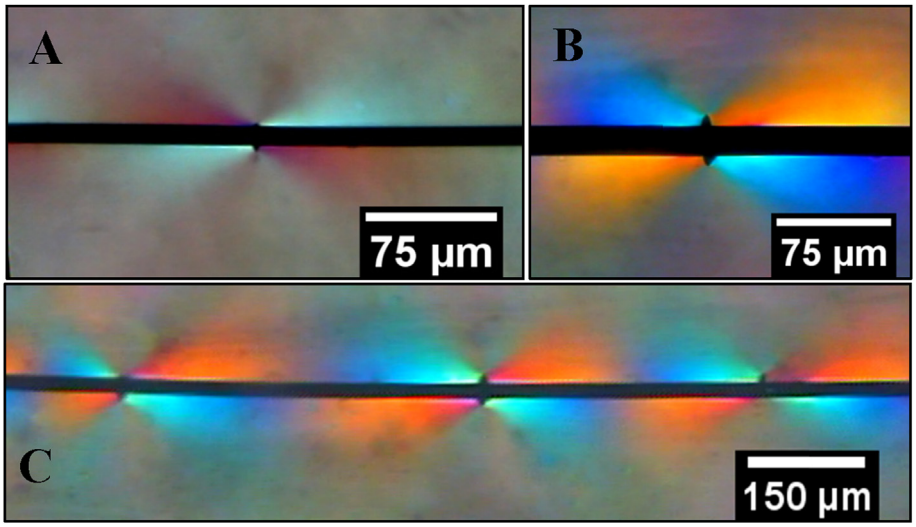

Fig. 9. Two high magnification optical micrographs of fiber fractures (A, B) and a large section of a SFFT sample showing several breaks along the fiber (C). Both examples shown here demonstrate crack propagation into the matrix, stressed regions around the fiber break, and interfacial damage along fiber.

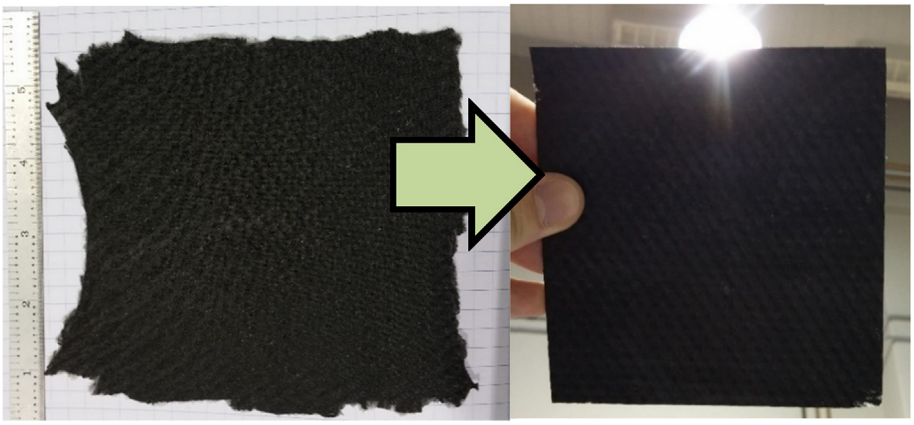

Fig. 10. (A) The resulting 14 cm by 14 cm composite from the VARTM system reduced to (B) the 13 cm by 13 cm composite after trimming.

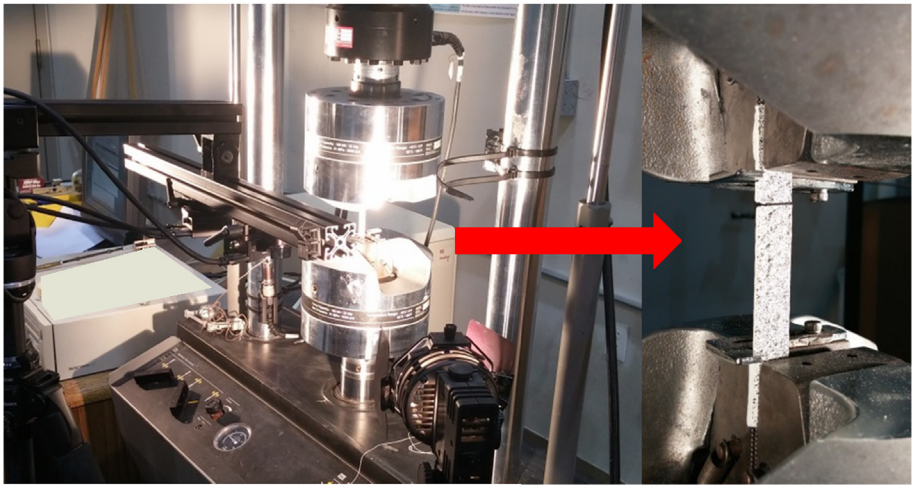

Fig. 11. (left) Testing set-up for DIC and tensile testing of composite samples and (right) a failed composite specimen.

Composite samples demonstrated an average failure strength of 85 MPa and average modulus of 9 GPa. The failure mode for the composite samples was either lateral or angled brittle failure in the gauge region as seen in Fig. 11 [10]. This type of failure indicates a high interfacial shear strength relative to fiber strength whereas a composite with an extremely high fiber strength relative to its interfacial shear strength tends to show explosive failure modes with failure largely along the fibers [36]. Having composites with non-explosive failures are preferable so that composite materials do not catastrophically fail.

The Voigt model (or rule of mixtures) is used to estimate the composite modulus based on volume fraction of fibers and carbon fiber properties along fiber axis. For the composite shown in Fig. 10, the composite modulus, E_{11}, is estimated to be 15.3 GPa using Eq. (4),

$$E_M V_M + E_F V_F = E_c \tag{4}$$

where V_f is fiber volume, E_f is fiber modulus, V_m is matrix volume, E_m is matrix modulus, and E_c is composite modulus. E_f and V_f are determined from the single fiber properties and density. Vf is calculated using the known mass of epoxy and fiber used in conjunction with the material densities to determine the volume of each component. E_m and V_m are determined using properties reported by the manufacturer. Experiments indicate a value of 9 GPa as per Table 3 and the lower observed value is expected due to a lack of highly aligned and continuous carbon fibers in the laminate. Fracture surfaces of the failed composite samples are visible in Fig. 12. It appears that the composites had a brittle fracture due to the relatively low strength of the fibers. Pores throughout the matrix, as seen in Fig. 12(b), are mostly present due to fiber pullout. These pores are located around other fibers and have the same diameter and therefore the authors conclude these are formed from fiber pullout.

Manufactured composites were produced in non-optimal conditions due to misalignment of the fibers in the preform during VARTM. The produced lignin carbon fiber was cut from a spool and therefore fiber plies were loose non-woven mats. Subsequently, it was difficult to achieve 100% fiber alignment. In addition, most fibers were non-continuous and voids were introduced during the VARTM process, although efforts were made to minimize defects. These factors affected the panel quality, led to out of plane

Table 3
The mechanical results for lignin carbon fiber composite using VIC-3D and MTS858.

$\mu \pm \sigma$	Failure Stress (MPa)	Failure Strain	Modulus (GPa)
Samples	MPa	mm/mm	GPa
6	85.0 ± 11.5	0.0094 ± 0.001	9.1 ± 0.6

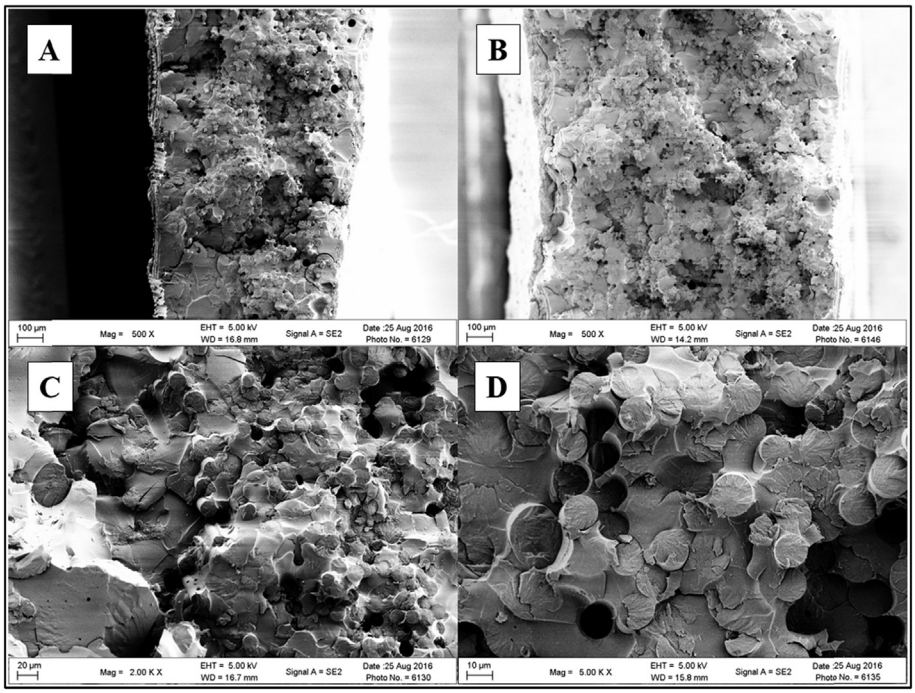

Fig. 12. Fracture surfaces of composite samples. A and B are 500X, C is 2.0 KX, and D is 5.0 KX.

deformation during tensile testing, and premature failure. Currently, panel production and quality is under continued development to address these needed areas of improvement.

Continued development in the mechanical properties of the lignin carbon fiber would also dramatically improve the overall composite performance as composite properties are a culmination of mechanical, interfacial, and structural properties [37,38]. Present investigations are under way to improve the graphitic structure of lignin fibers, reduce fiber defects, optimize biomass precursors, modifying the extrusion equipment to handle lignin volatiles, and increase temperatures and/or modify temperature cycles during stabilization/carbonization. Lignin based carbon fiber composites are suitable for non-structural and semi-structural applications, but increasing modulus and failure stress of the fibers further will enable structural composites by taking advantage of lignin carbon fiber's superior matrix interaction.

4. Conclusion

Organosolv fractionated lignin carbon fiber was produced and characterized via Nano-UTM, Single Fiber Fragmentation, and X-Ray Diffraction. In addition, a unidirectional carbon fiber reinforced polymer composite was manufactured with the lignin carbon fiber through a modified VARTM process. Lignin carbon fiber exhibited little to no surface defects from SEM and optical microscopy. Mechanical results for the carbon fiber indicated an average modulus close to 36 GPa and failure stress of ~600 MPa (3.66 and 630 MPa shape and scale parameters). Interfacial shear strength values were relatively high around ~16 MPa for unsized lignin carbon fiber. SFFT saturated samples revealed fiber fractures propagating into the matrix and no fiber pullout. These interface strength results indicate that lignin carbon fiber would be ideal for applications that take advantage of interfacial strengths such as chopped fiber composites or fillers. XRD results and analysis demonstrated little to no crystalline regions in the fibers, which is likely the reason for low modulus of the fibers compared to commercially available PAN based fibers. Nevertheless, lignin based carbon fibers tend to follow the same strain hardening trend found in other carbon fibers, which may indicate a general rearrangement of amorphous carbon when strain is applied. After the lignin carbon fiber was fully characterized, unidirectional mats were placed in a preform inside a VARTM system and produced into a composite. Fiber alignment and quantity varied across the panel during production. The composite panel mechanical properties were ~9 GPa and ~85 MPa for modulus and failure strength, respectively. Composite samples demonstrated lateral brittle failures in the gage region indicating a large ratio of interface to mechanical strength. Produced lignin carbon fiber composites exhibited non-explosive failure mechanisms with minimal fiber pullout as seen in SFFT.

Overall, the lignin carbon fiber demonstrated acceptable mechanical and interfacial properties for potential applications in chopped carbon fiber composites for structural applications. This advantage of lignin based carbon fiber over commercial PAN based carbon fibers (that require additional sizing) suggests that lignin carbon fiber would be preferable in some applications that mobilize the interface such as discontinuous fiber based composites, fused deposition modeling for additive manufacturing, and fillers. Results presented in this study are a significant improvement to current lignin carbon fiber characterization techniques and lignin carbon fiber composite manufacturing. Continued development and improvement of the mechanical performance will open more utilization of lignin carbon fiber, particularly in automotive applications.

Acknowledgements

We'd like to acknowledge TennEra, L.L.C. (www.tennera.com) for supporting this research project, Dr. Joseph Spruiell for his aid in XRD analysis, Dr. Joseph Bozell and Alexandra Peeden for their help with molecular weight determination, and Valeria Garcia-Negron for assisting with thermal characterization of the lignin. In addition, we'd also like to thank Dr. Ahmad Vakili for his contributions

in thermal processing lignin fibers. Dr. Penumadu would like to acknowledge the support of the Solid Mechanics Program of the US Office of Naval Research through ONR Contract N00014710504 under a program managed by Dr. Yapa Rajapakse and is gratefully acknowledged.

References

[1] 2017 and later model year light-duty vehicle greenhouse gas Emissions and corporate average fuel economy standards, in: Federal Register, US Environmental Protection Agency, 2012, pp. 63200–63624.
[2] D.A. Baker, T.G. Rials, Recent advances in low-cost carbon fiber manufacture from lignin, J. Appl. Polym. Sci. 130 (2) (2013) 713–728.
[3] M.M.R. Khan, et al., Carbon fiber from natural biopolymer Bombyx mori silk fibroin with iodine treatment, Carbon 45 (5) (2007) 1035–1042.
[4] A. Sluiter, et al., Determination of Structural Carbohydrates and Lignin in Biomass, National Renewable Energy Laboratory, 2008.
[5] D.A. Baker, N.C. Gallego, F.S. Baker, On the characterization and spinning of an organic-purified lignin toward the manufacture of low-cost carbon fiber, J. Appl. Polym. Sci. 124 (1) (2012) 227–234.
[6] L.M.W.K. Gunaratne, R.A. Shanks, Melting and thermal history of poly(hydroxybutyrate-co-hydroxyvalerate) using step-scan DSC, Thermochim. Acta 430 (1–2) (2005) 183–190.
[7] R.J. Sammons, et al., Characterization of organosolv lignins using thermal and FT-IR spectroscopic analysis, BioResources 8 (2) (2013) 2752–2767.
[8] P. Liu, et al., Glass transition temperature of starch studied by a high-speed DSC, Carbohydr. Polym. 77 (2) (2009) 250–253.
[9] Super Sap 100/1000 Technical Data Sheet, 2010. Available from: https://entropyresins.com/wp-content/uploads/2014/03/TDS_100_1000_v4-TDS-100-1000-System.pdf.
[10] International A, ASTM D3039: Standard Test Method for Tensile Properties of Polymer Matrix Composite Materials, 2014.
[11] M. Kant, D. Penumadu, Dynamic mechanical characterization for nonlinear behavior of single carbon fibers, Compos. Part A Appl. Sci. Manuf. 66 (2014) 201–208.
[12] Hunston, D., et al., Test Protocol for Single-fiber Fragmentation Test - International Round Robin.
[13] S. Feih, et al., Establishing a Testing Procedure for the Single Fiber Fragmentation Test, 2004.
[14] A.N. Netravali, et al., Interfacial shear strength studies using the single-filament-composite test. I: experiments on graphite fibers in epoxy, Polym. Compos. 10 (4) (1989) 226–241.
[15] B.E. Warren, P. Bodenstein, The shape of two-dimensional carbon black reflections, Acta Cryst. 20 (602) (1966).
[16] J.-B. Donnet, R.C. Bansal, Carbon Fibers (1990) 85–160.
[17] H. Klug, L. Alexander, X-Ray Diffraction Procedures for Polycrystalline and Amorphous Materials, 1974.
[18] B.E. Warren, X-ray Diffraction, Reading, Mass.: Addison-Wesley Pub. Co, 1969.
[19] S. Van der Zwaag, The concept of filament strength and Weibull modulus, J. Test. Eval. 17 (5) (1989) 292–298.
[20] D. Wilson, Statistical tensile strength of NextelTM 610 and NextelTM 720 fibres, J. Mater. Sci. 32 (10) (1997) 2535–2542.
[21] C. Beetz, A self consistent Weibull Analysis of carbon fiber strength distributions, Fibre Sci. Technol. 16 (1982) 81–94.
[22] K. Naito, et al., Tensile and flexural properties of single carbon fibers, in: ICCM-18, 2011 (Jeju Island, S. Korea).
[23] Y. Nordström, R. Joffe, E. Sjöholm, Mechanical characterization and application of Weibull statistics to the strength of softwood lignin-based carbon fibers, J. Appl. Polym. Sci. 130 (5) (2013) 3689–3697.
[24] J.F. Kadla, et al., Lignin-based carbon fibers for composite fiber applications, Carbon 40 (2002) 2913–2920.
[25] J. Lin, et al., Improvement of mechanical properties of softwood lignin-based carbon fibers, J. Wood Chem. Technol. 34 (2) (2013) 111–121.
[26] Y. Liu, H.G. Chae, S. Kumar, Gel-spun carbon nanotubes/polyacrylonitrile composite fibers. Part III: effect of stabilization conditions on carbon fiber properties, Carbon 49 (13) (2011) 4487–4496.
[27] X. Huang, Fabrication and properties of carbon fibers, Materials 2 (4) (2009) 2369–2403.
[28] A. Beste, ReaxFF study of the oxidation of lignin model compounds for the most common linkages in softwood in view of carbon fiber production, J. Phys. Chem. A 118 (5) (2014) 803–814.
[29] H. Chung, N.R. Washburn, Chemistry of lignin-based materials, Green Mater. 1 (3) (2013) 137–160.
[30] C. Lew, et al., The effect of silica (SiO_2) nanoparticles and ammonia/ethylene plasma treatment on the interfacial and mechanical properties of carbon-fiber-reinforced epoxy composites, J. Adhes. Sci. Technol. 21 (14) (2007) 1407–1424.
[31] B.W. Kim, J.A. Nairn, Observations of fiber fracture and interfacial debonding phenomena using the fragmentation test in single fiber composites, J. Compos. Mater. 36 (15) (2002) 1825–1858.
[32] J. Zhao, et al., A comparative study of fibre/matrix interface in glass fibre reinforced polyvinylidene fluoride composites, Colloids Surf. A Physicochem. Eng. Asp. 413 (2012) 58–64.
[33] J.M. Park, Interfacial properties of two-carbon fiber reinforced polycarbonate composites using two-synthesized graft copolymers as coupling agents, J. Colloid Interface Sci. 225 (2) (2000) 384–393.
[34] K. Sudo, K. Shimizu, A new carbon Fiber from lignin, J. Appl. Polym. Sci. 44 (1992) 127–134.
[35] I. Brodin, et al., Oxidative stabilisation of kraft lignin for carbon fibre production, Holzforschung (2) (2012) 66.
[36] O.I. Okoli, G.F. Smith, Failure modes of fibre reinforced composites: the effects of strain rate and fibre content, J. Mater. Sci. 33 (1998) 5415–5422.
[37] X. Yan, et al., Relationship study between crystal structure and thermal/mechanical properties of polyamide 6 reinforced and unreinforced by carbon fiber from macro and local view, Polymer 55 (23) (2014) 6186–6194.
[38] N. Lu, R.H. Swan, I. Ferguson, Composition, structure, and mechanical properties of hemp fiber reinforced composite with recycled high-density polyethylene matrix, J. Compos. Mater. 46 (16) (2011) 1915–1924.